



Cite this: *Green Chem.*, 2014, **16**, 3951

## Enhanced hydrogenation of ethyl levulinate by Pd-AC doped with Nb<sub>2</sub>O<sub>5</sub>†

Feiyang Ye, Damin Zhang, Teng Xue, Yimeng Wang and Yejun Guan\*

Gamma-valerolactone (GVL), as sustainable feedstock for high-value chemicals and fuel, has been produced by hydrogenation of levulinic acid (LA) or ethyl levulinate (EL). In this work, Pd nanoparticles supported on Nb<sub>2</sub>O<sub>5</sub>-doped activated carbon (AC) were prepared *via* wet incipient impregnation with PdCl<sub>2</sub> followed by reduction with NaBH<sub>4</sub>. The dispersed niobia plays a bifunctional role in the catalytic process: stabilizing Pd nanoparticles and acting as an acidic co-catalyst. This synergistic effect between niobia and Pd leads to an unprecedented high activity of supported Pd catalysts in EL hydrogenation. The synergy is correlated with both the niobia loading and calcination temperature, with 10 wt% Nb<sub>2</sub>O<sub>5</sub> calcined at 500 °C showing the best performance (EL conversion of 87% and GVL selectivity of 97%) under mild reaction conditions (100 °C and 0.5 MPa H<sub>2</sub>).

Received 27th May 2014,  
Accepted 18th June 2014

DOI: 10.1039/c4gc00972j

www.rsc.org/greenchem

### Introduction

Cellulosic biomass is a vast and renewable resource that serves as feedstock to produce both chemicals and fuels.<sup>1,2</sup> In the near future, catalytic conversion of biomass to a variety of chemicals will drastically change the energy-base from fossil to renewable feedstock. In this context, many carbohydrate-derived compounds from lignocellulosic biomass are highly applicable and could be widely utilized. For example, it is possible to produce ethanol and other platform chemicals, such as levulinate ester, levulinic acid and 5-hydroxymethyl-furfural (HMF) from glucose monomers obtained from lignocellulose.<sup>3</sup> Further hydrogenation of levulinate ester or levulinic acid then leads to the formation of  $\gamma$ -valerolactone (GVL), which is a highly stable and low toxic compound.<sup>4</sup> This compound has been widely used as a fuel,<sup>5</sup> a fuel additive,<sup>6</sup> an intermediate for the production of chemicals,<sup>7–11</sup> and a renewable solvent.<sup>6,12,13</sup> Therefore, the production and application of GVL have attracted much attention in catalysis.<sup>4,11,13–27</sup> Both homogeneous<sup>28</sup> and heterogeneous<sup>29–32</sup> catalysts have been extensively explored.

To date, most studies have mainly focused on the conversion of LA as a precursor. Manzer and coworkers systematically investigated the catalytic activity of various metals (*e.g.* Ir, Rh, Pd, Ru, Pt, Re and Ni) supported on AC at 150 °C under 800 psi H<sub>2</sub> for 2 h.<sup>11,33</sup> Of the catalysts studied, Ru-C was

noticeably the most active one which gave a LA conversion of 80%. By further optimization, complete LA conversion was obtained with the GVL selectivity exceeding 95%. Compared with Ru, Pt and Pd were reported to be much less active for GVL production, giving a moderate LA conversion.

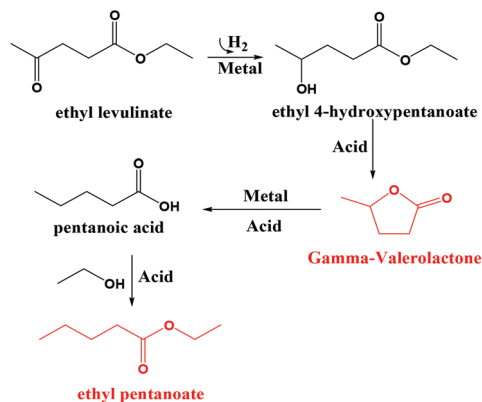
LA is generally produced from lignocellulose in aqueous acid medium, wherein polymeric humin is always formed by the thermal decomposition of intermediates, therefore leading to a low yield of LA.<sup>34–37</sup> The humin formation can be significantly inhibited in the presence of alcohols, resulting in the formation of the corresponding levulinic esters in high yield (95%) compared with LA (25%) from C6 sugars.<sup>38</sup> A 75% yield of methyl levulinate could be obtained directly from cellulose with a mixed-acid system consisting of both Lewis and Brønsted acids.<sup>39</sup> Li and coworkers<sup>40</sup> reported an economical pathway for the production of pure levulinate esters from cellulose. An optimized yield of around 50% was achieved at 210 °C for 120 min with a very low sulfuric acid concentration (0.01 M) and an initial cellulose concentration below 100 g L<sup>-1</sup>. In fact, the easier separation of levulinate esters from the reaction mixture and developing techniques to increase the recovery efficiency of alcohols during the synthesis will make the production of levulinate esters economically favorable. Therefore the catalytic hydrogenation of levulinic esters to GVL may show great commercial potential due to suppression of active metal leaching of hydrogenation catalysts caused by free carboxyl of LA.<sup>39,40</sup>

Nadgeri *et al.*<sup>41</sup> reported the liquid-phase hydrogenation of methyl levulinate over graphite- and zeolite-supported ruthenium catalysts and the mixture of graphite-supported ruthenium metal catalysts and zeolite in water. Two reaction pathways were found: direct hydrogenation to  $\gamma$ -valerolactone

Shanghai Key Laboratory of Green Chemistry and Chemical Processes, East China Normal University, North Zhongshan Road 3663, 200062 Shanghai, China.

E-mail: yjguan@chem.ecnu.edu.cn; Fax: +86-21 32530334

†Electronic supplementary information (ESI) available. See DOI: 10.1039/c4gc00972j



Scheme 1 Conversion of ethyl levulinate to ethyl pentanoate.

and hydrogenation of carbonyl groups to methyl 4-hydroxyvalerate. The latter compound undergoes dealcoholization to form  $\gamma$ -valerolactone. From Scheme 1, one can clearly see that the presence of zeolites may enhance the dealcoholization step. This promotion effect of acidic materials has also been observed in LA hydrogenation using USY, Amberlyst-15, HZSM-5, and  $\beta$ -zeolite.

Recently, Xiong *et al.* developed a  $\text{Nb}_2\text{O}_5/\text{C}$  composite, which showed high activity in the conversion of glucose to 5-hydroxymethylfurfural.<sup>42</sup> Moreover, the carbon-loaded oxide composites showed improved hydrothermal stability,<sup>43</sup> which is of great advantage regarding biomass conversion. When Pd was supported on the obtained  $\text{Nb}_2\text{O}_5/\text{C}$  composite, GVL can be successfully hydrogenated to pentanoic acid. Inspired by these findings, herein we systematically studied the synergy between Pd and  $\text{Nb}_2\text{O}_5$  in hydrogenation of EL to GVL and PE. We demonstrated that the addition of niobia significantly improved the acidity of Pd/AC catalysts, leading to a fast hydrogenation and dealcoholization in the overall process. Consequently, the EL can be converted to GVL under mild reaction conditions.

## Experimental

### Preparation of niobia-carbon supports

Niobia-carbon supports with various loading from 0 to 20 wt%  $\text{Nb}_2\text{O}_5$  were prepared by incipient impregnation. Active carbon was purchased from STREM Chemicals and was dried before use. A typical preparation of supports (10 wt% niobia loading) involved the use of 2.61 g of active carbon which was mixed with niobium oxalate hydrate (0.607 g) dissolved in 5 ml of  $\text{H}_2\text{O}$ . After being dried at 60 °C for 12 h, the sample was calcined at 500 °C for 2 h with a ramp rate of 3 °C  $\text{min}^{-1}$  under a  $\text{N}_2$  flow. The sample was denoted  $x\text{Nb}-y\text{AC}$  ( $x$  stands for niobia loading,  $y$  stands for the calcination temperature).

### Preparation of the Pd-niobia-carbon catalyst

The Nb-AC composites were used to load Pd with a loading of 3 wt% *via* a deposition-precipitation method. In a typical

synthesis (3Pd-10Nb-500-AC), 0.291 g of the 10Nb-500-AC support was distributed in 75 ml of  $\text{H}_2\text{O}$  with stirring for 2 h. An appropriate amount of  $\text{H}_2\text{PdCl}_4$  aqueous solution was added to the solution. After being stirred for 2 h, 0.6 ml of 1 M NaOH aqueous solution was added to the mixture. Then, a  $\text{NaBH}_4$  aqueous solution was added into the suspension as the reducing reagent ( $\text{NaBH}_4/\text{Pd} = 10$ , molar ratio) with stirring for 5 h. The slurry was filtered, washed with deionized water, and finally dried at 60 °C for 24 h. For comparison, the catalytic activity of a commercial catalyst, *i.e.*, 5 wt% Pd-C from Alfa-Aesar was tested.

### Preparation of the Pd-niobia catalyst

For comparison, pure niobia supported Pd catalysts were prepared by the same deposition-precipitation method. The niobia supports included a commercial niobia ( $\text{Nb}_2\text{O}_5\text{-COM}$ ) purchased from Alfa-Aesar, and two other niobia samples prepared with calcination of niobium oxalate at 300 and 500 °C for 2 h (denoted  $\text{Nb}_2\text{O}_5\text{-300}$  and  $\text{Nb}_2\text{O}_5\text{-500}$ , respectively).

### Catalyst characterization

Nitrogen adsorption-desorption isotherms at -196 °C were obtained using BELSORP-Max equipment. Prior to the measurement, the samples were first degassed at 150 °C under vacuum for 6 h. Specific surface areas were calculated according to the BET-method using five relative pressure points at an interval of 0.05–0.30. The pore size distribution was obtained by the BJH model applied to the adsorption branch of the isotherm.

Pulse CO chemisorption was performed on a Micromeritics AutoChem 2910 to determine the metal dispersion of the reduced catalysts. Prior to measurement, 100 mg catalyst was reduced in a flow of 100  $\text{mL min}^{-1}$  10 vol%  $\text{H}_2$  in Ar at 200 °C for 2 h and then flushed in He for 2 h. After being cooled to 30 °C in He, the CO gas pulses (5 vol% in He) were introduced in a flow of 100  $\text{ml min}^{-1}$ . The changes in the CO gas phase concentration were followed by a thermal conductivity detector (TCD).

The acidities of the supports were characterized by  $\text{NH}_3$  temperature-programmed desorption (TPD) recorded on a TP-5080 (Tianjin Xianquan, China) equipped with TCD. Before the TPD experiments, the samples were pretreated under a helium flow of 25  $\text{mL min}^{-1}$  at 500 °C for 2 h. The physisorbed  $\text{NH}_3$  was removed by flowing helium at 100 °C until a stable signal was obtained. Desorption of strongly adsorbed  $\text{NH}_3$  was performed by heating the catalyst at a rate of 10 °C  $\text{min}^{-1}$  under flowing helium (25  $\text{mL min}^{-1}$ ), from room temperature to 500 °C.

The powder X-ray diffraction (XRD) patterns were collected on a Rigaku Ultima IV X-ray diffractometer using  $\text{Cu K}\alpha$  radiation ( $\lambda = 1.5405 \text{ \AA}$ ) operated at 35 kV and 25 mA. Scanning electron microscopy (SEM) equipped with an energy dispersive X-ray analysis (EDX) unit (Oxford, UK) was performed on a Hitachi S-4800 microscope. Transmission electron microscopy (TEM) images were taken on a FEI Tecnai G<sup>2</sup> F30 microscope operating at 300 kV.

## Catalytic activity measurements

Catalytic reactions for conversion of ethyl levulinate to  $\gamma$ -valerolactone were conducted in a Teflon-lined (100 mL) steel batch reactor at a stirring speed of 800 rpm for 5 h. The typical hydrogenation conditions were: 100 °C; 10 ml of 0.25 M ethyl levulinate aqueous solution; 25 mg of catalyst; and H<sub>2</sub> pressure 0.5 MPa. Once the reactor was cooled down to room temperature, the products were analyzed with an FID detector and a capillary column DB-Wax. The following temperature program method was used for GC analysis: 120 °C for 16 min and then heated to 220 °C with a ramp rate of 20 °C min<sup>-1</sup> and kept at 220 °C for another 9 min.

## Results and discussion

### Catalyst characterization

Fig. 1 shows the XRD patterns of the niobia-carbon supports calcined at 300, 500 and 700 °C. Some unidentified diffraction peaks were observed on the commercial AC, which might be ascribed to impurities. Except for these peaks, no extra peak was seen for the supported niobia species when calcined at 300 or 500 °C, meaning that Nb<sub>2</sub>O<sub>5</sub> were highly dispersed in the amorphous phase. Previous studies have shown that niobium oxalate can be completely decomposed by calcination at around 300 °C.<sup>47,48</sup> In contrast, the 10Nb-700-AC catalyst showed several diffraction peaks at 22 and 28° corresponding to the diffractions of the hexagonal TT-Nb<sub>2</sub>O<sub>5</sub> phase (JCPDS [07-0061]).<sup>29</sup>

The textural properties of AC and Nb<sub>2</sub>O<sub>5</sub> doped AC, including BET specific surface area (SSA), total pore volume ( $V_{\text{total}}$ ) and the pore size are summarized in Table 1. Similar N<sub>2</sub> adsorption isotherms (Type I) were observed for all AC based materials (Fig. S1 in ESI†), which are characteristic of mesoporous materials. Loading Nb<sub>2</sub>O<sub>5</sub> led to a gradual decrease of surface area from 1204 (AC) to 926 m<sup>2</sup> g<sup>-1</sup> (20 wt% Nb<sub>2</sub>O<sub>5</sub>-AC). It should be noted that the calcination temperature also affected the surface area. The surface areas of 10Nb- $y$ -AC ( $y = 300, 500, \text{ and } 700$  °C) supports are 956, 1116, 1205 m<sup>2</sup> g<sup>-1</sup>,

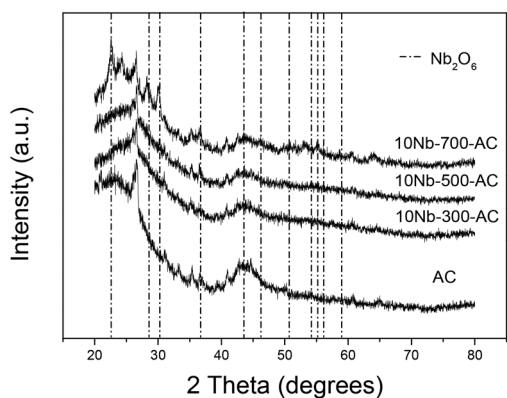


Fig. 1 XRD patterns of 10Nb- $y$ -AC supports calcined at different temperatures ( $y = 300, 500, \text{ and } 700$  °C).

Table 1 N<sub>2</sub> adsorption data of the  $x\text{Nb}-y\text{-AC}$  materials

Sample	$S_{\text{BET}}$ (m <sup>2</sup> g <sup>-1</sup> )	$V_{\text{total}}$ (cm <sup>3</sup> g <sup>-1</sup> )	Pore size (nm)	$T_{\text{NH}_3}$ (°C)	Acid density (mmol g <sub>cat</sub> <sup>-1</sup> )
AC	1204	0.79	2.6	—	n.d. <sup>a</sup>
2.5Nb-500-AC	1184	0.75	2.5	—	—
5Nb-500-AC	1121	0.73	2.5	—	—
10Nb-500-AC	1116	0.71	2.5	245	0.097
20Nb-500-AC	926	0.57	2.4	230	0.17
10Nb-300-AC	956	0.60	2.5	200	0.29 <sup>b</sup>
10Nb-700-AC	1205	0.79	2.6	—	n.d.

<sup>a</sup> Not detected. <sup>b</sup> Pretreated at 300 °C.

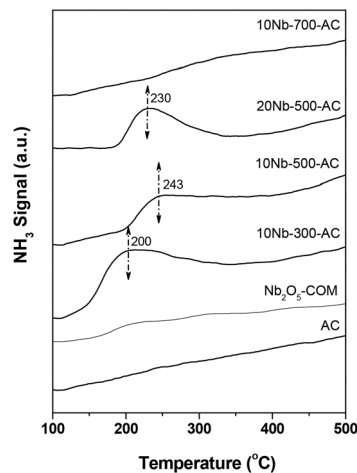


Fig. 2 NH<sub>3</sub>-TPD profiles of the supports.

respectively (Fig. S2 in ESI†). We surmise that the highly dispersed amorphous Nb<sub>2</sub>O<sub>5</sub> might block the mesopores to some extent and this blockage effect disappears when Nb<sub>2</sub>O<sub>5</sub> turns to bulk material. This phenomenon has also been observed by the Datye group.<sup>44</sup>

The acid densities of  $x\text{Nb}-y\text{-AC}$  materials calculated according to NH<sub>3</sub>-TPD experiments are also shown in Table 1 (Fig. 2). AC did not show any NH<sub>3</sub> desorption at temperatures higher than 100 °C. The Nb<sub>2</sub>O<sub>5</sub>-COM also showed very weak NH<sub>3</sub> desorption. The 10Nb-AC supports calcined at 300 and 500 °C gave acid densities of 0.29 and 0.097 mmol g<sup>-1</sup>, respectively. This means that the acid density of Nb<sub>2</sub>O<sub>5</sub> decreased during the calcination. In line with this finding, the 10Nb-AC calcined at 700 °C showed negligible desorption of NH<sub>3</sub>. Another important feature of acidity is the acidic strength which is revealed by the desorption peak of NH<sub>3</sub>. The maximum desorption peaks of 10Nb-AC calcined at 300 and 500 °C are about 200 and 245 °C, respectively. This result indicates that the niobia species calcined at 500 °C showed stronger acidity than that calcined at 300 °C as reported by Iizuka and co-workers.<sup>45,46</sup> The acidity of niobia is mainly attributed to its Brønsted acid sites and medium-strong Lewis acid sites due to its coordinatively unsaturated Nb<sup>5+</sup> species.<sup>47</sup> For the Nb-AC catalyst calcined at 500 °C, the 20Nb-500-AC contained more amounts of acid site (0.17 mmol g<sub>cat</sub><sup>-1</sup>) due to higher niobia

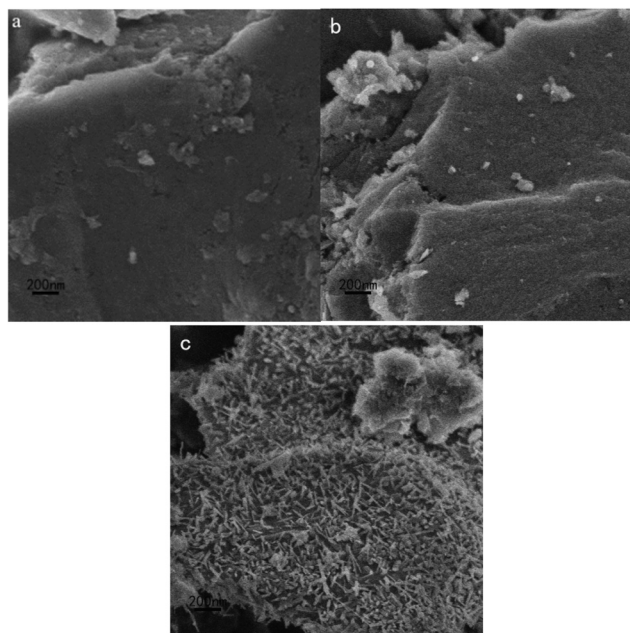


Fig. 3 SEM images of 10Nb-*y*-AC supports calcinated at different temperatures: (a) 300 °C; (b) 500 °C; (c) 700 °C.

loading. The maximum NH<sub>3</sub> desorption temperature of 20Nb-500-AC was about 230 °C, slightly lower than that of 10Nb-500-AC.

SEM images (Fig. 3) show that morphologies of supports were similar to each other when the calcination temperature did not exceed 500 °C. The EDX data (Table S1 in ESI†) recorded in different zones of the 10Nb-500-AC support (Fig. S3 in ESI†) suggested that the Nb<sub>2</sub>O<sub>5</sub> was indeed well-dispersed on AC without any aggregation. Interestingly, slice-like and rod-like structures were clearly observed for the sample calcined at 700 °C. Nowak *et al.*<sup>47</sup> reported that Nb<sub>2</sub>O<sub>5</sub> had strong mobility, which will explain the crystallization of niobia on the 10Nb-700-AC support.

Fig. 4 displays the XRD patterns of the Pd-*x*Nb-*y*-AC catalysts. The diffraction peak at 40° is due to the (111) reflection of Pd nanoparticles. The peak intensity became weaker with the increase of Nb<sub>2</sub>O<sub>5</sub> content, indicating that Pd nanoparticles are well dispersed on Nb<sub>2</sub>O<sub>5</sub> attributed to the so-called strong metal-support interaction (SMSI). Fig. 5 shows the typical TEM images of supported Pd catalysts. No visible Pd particles were found, consistent with that of XRD. Thus the accurate size of Pd cannot be determined by XRD and TEM. The supported Pd catalysts were subjected to CO chemisorption measurements and the results are shown in Table 2. The dispersions of Pd nanoparticles on 3Pd-AC, 3Pd-2.5Nb-500-AC, 3Pd-5Nb-500-AC, 3Pd-10Nb-500-AC, 3Pd-20Nb-500-AC, 3Pd-10Nb-300-AC and 3Pd-10Nb-700-AC are 53%, 56%, 59%, 65%, 78%, 35%, and 52%, respectively. Apparently the presence of Nb<sub>2</sub>O<sub>5</sub> indeed benefits the loading of Pd and results in very fine Pd particles with a diameter of about 1.4 nm. Furthermore, the calcination temperature of Nb<sub>2</sub>O<sub>5</sub> greatly influences

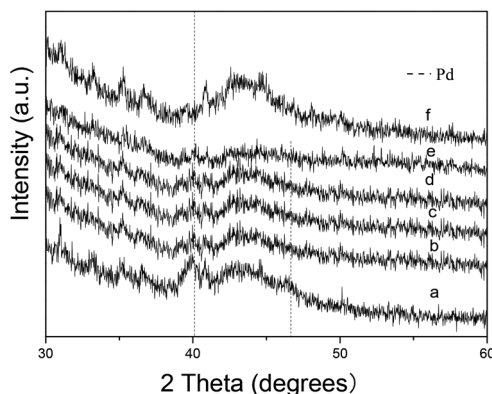


Fig. 4 XRD patterns of pure AC and Pd-*x*Nb-500-AC catalysts with various niobia loadings: (a) 3Pd-AC; (b) 3Pd-2.5Nb-500-AC; (c) 3Pd-5Nb-500-AC; (d) 3Pd-10Nb-500-AC; (e) 3Pd-20Nb-500-AC; and (f) AC.

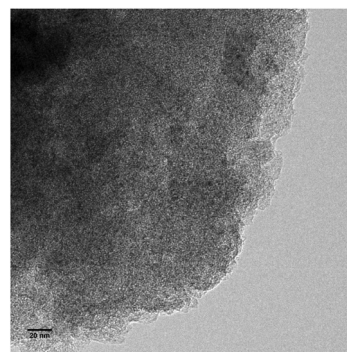


Fig. 5 TEM image of 3Pd-10Nb-500-AC (scale bar: 20 nm).

Table 2 CO chemisorption for the Pd-*x*Nb-*y*-AC catalysts

Sample	Dispersion (%)	<i>D</i> <sub>Pd</sub> (nm)
3Pd-AC	53(32 <sup>a</sup> )	2.1(3.5 <sup>a</sup> )
3Pd-2.5Nb-500-AC	56	2.0
3Pd-5Nb-500-AC	59	1.9
3Pd-10Nb-500-AC	65(59 <sup>b</sup> )	1.7(1.9 <sup>b</sup> )
3Pd-20Nb-500-AC	78	1.4
3Pd-10Nb-300-AC	35	3.2
3Pd-10Nb-700-AC	52	2.2

<sup>a</sup> Used for five times. <sup>b</sup> Used for six times.

the dispersion of Pd nanoparticles, with 500 °C being the best one.

### Catalyst performance of EL hydrogenation with different niobia contents

The hydrogenation activities of ethyl levulinate to  $\gamma$ -valerolactone on 3Pd-*x*Nb-500-AC are listed in Table 3. Commercial Pd-AC exhibited the lowest activity with a GVL yield of 21%. Similarly, 3 wt% Pd-AC also gave a low yield of 28%. It should be noted that two side-products, namely LA and ethyl 4-hydroxypentanoate (EHP) were also detected in varying amounts

**Table 3** EL hydrogenation on supported Pd catalysts

Catalyst <sup>a</sup>	Conv. (%)	Sel. (%)			TOF <sup>b</sup>
		LA	GVL	EHP	
5Pd-AC <sup>c</sup>	30	7	70	23	0.19
3Pd-AC	38	3	74	23	0.25
3Pd-2.5Nb-500-AC	68	3	93	4	0.44
3Pd-5Nb-500-AC	74	3	94	3	0.48
3Pd-10Nb-500-AC	87	2	93	5	0.57
3Pd-20Nb-500-AC	83	4	92	4	0.53
3Pd-10Nb-300-AC	61	4	92	4	0.39
3Pd-10Nb-700-AC	68	3	79	18	0.43
3Pd-AC + 10Nb-300-AC <sup>d</sup>	57	4	94	2	—
3Pd-AC + 10Nb-500-AC <sup>d</sup>	57	2	92	6	—
3Pd-AC + 10Nb-700-AC <sup>d</sup>	53	3	85	12	—

<sup>a</sup> Reaction conditions: 10 ml of 0.25 M EL aqueous solution; 0.5 MPa H<sub>2</sub>; 100 °C; 25 mg catalyst (3 wt% Pd); 5 h; 800 rpm. <sup>b</sup> The TOF is defined as mol<sub>GVL+EHP</sub> g<sub>Pd</sub><sup>-1</sup> h<sup>-1</sup>. <sup>c</sup> 5Pd-AC catalyst was purchased from Alfa-Aesar, 15 mg. <sup>d</sup> Physical mixture of 25 mg 3Pd-AC and 25 mg 10Nb-*y*-AC.

depending on the nature of the AC used. The selectivity to EHP on commercial 5 wt% Pd-AC was as high as 23%, meanwhile it was also observed as the main side-product (selectivity of 23%) on home-made 3 wt% Pd-AC. The very similar selectivity to EHP is probably determined by the thermodynamics of the dealcoholization from EHP to GVL in the absence of acid catalysts. The formation of LA might be ascribed to the hydrolysis of EL in aqueous solution. With 2.5 wt% Nb<sub>2</sub>O<sub>5</sub> loaded on AC, an EL conversion of 68% and a GVL selectivity of 93% were achieved on 3Pd-2.5Nb-500-AC. The activities went up along with the increase of niobia content. The highest yield of GVL (81%) was obtained on the 3Pd-10Nb-500-AC catalyst. The TOF based on Pd loading is calculated to be 0.57 (mol<sub>GVL</sub> g<sub>Pd</sub><sup>-1</sup> h<sup>-1</sup>). This value is close to previous reports on Pd/SiO<sub>2</sub> and Pd/CNT catalysts under a much harsher condition for the hydrogenation of LA, wherein higher temperature (140–200 °C) and higher H<sub>2</sub> pressure (30–90 bar) were employed.<sup>48,49</sup> This result clearly demonstrates the advantage of using EL as the starting compound to produce GVL in biomass transformation. To clarify the difference in supported Pd catalysts in EL and LA hydrogenation, we have compared the catalytic activity of Pd-AC and Pd-Nb-AC in LA and EL hydrogenation (Table S2 in ESI†). The conversion of LA and EL on the Pd-AC catalyst was 20% and 38%, respectively. The relative lower hydrogenation activity of LA might be ascribed to the strong adsorption ability of the carboxylate group on Pd nanoparticles, which has been reported in some hydrogenation reactions involving HCOOH.<sup>23</sup> On the Pd-Nb-AC catalyst, the EL and LA conversion was 87% and 62%, respectively. This result may be explained by the effect of Nb<sub>2</sub>O<sub>5</sub> as an acidic promoter in hydrogenating carbonyl bonds.<sup>16</sup>

#### Catalyst performance of EL hydrogenation with different calcination temperatures of niobium oxide

Also shown in Table 3 are the EL conversions on Pd-10Nb-*y*-AC (*y* = 300, 500, and 700). The GVL conversion over the

3Pd-10Nb-500-AC catalyst was 87%, which was higher than those of 3Pd-10Nb-300-AC (61%) and 3Pd-10Nb-700-AC (68%). This result emphasized the importance of calcination temperature in governing the catalytic activity of the Pd-Nb-AC catalyst. The niobia phase changed from amorphous to crystalline when calcination temperature increased from 300 to 700 °C. This change may affect the electronic properties of supported Pd and also the acidic properties of the catalysts. The lower EL conversion on Pd-10Nb-300-AC might be due to the larger Pd particles (3.4 nm), whereas the presence of bulk Nb<sub>2</sub>O<sub>5</sub> (Fig. 2) may be responsible for the activity decrease of Pd-10Nb-700-AC which is consistent with the activities of Pd supported on bulk Nb<sub>2</sub>O<sub>5</sub> catalysts (Table S3 in ESI†). On the bulk Nb<sub>2</sub>O<sub>5</sub> support, no XRD diffraction of Pd was observed (Fig. S4 in ESI†), meaning the Pd species were well dispersed. To shed more light on the interaction of Pd and niobia on the hydrogenation activity, we have compared the reactivity of physical mixtures of Pd-AC and 10Nb-*y*-AC (Table 3). The EL conversion on the Pd-AC catalyst increased from 38% to 57% in the presence of 10Nb-*y*-AC (*y* = 300 and 500). The promotion effect is weakened for 10Nb-700-AC. These results suggest that the 10Nb-*y*-ACs were indeed involved in the hydrogenation process. However the activities of the physical mixtures were lower than their counterparts with close interactions between Pd and niobia, namely, Pd-10Nb-*y*-ACs, pointing to the synergistic effect of Pd and niobia on AC. It is worth noting that the bulk Nb<sub>2</sub>O<sub>5</sub> is probably not in favor of strong Pd-Nb<sub>2</sub>O<sub>5</sub> interaction.

It is clearly seen that the Nb-*y*-AC supports were involved in the overall hydrogenation process. To clarify the role of Nb-*y*-AC in the process, we compared the performance of 10Nb-*y*-AC and AC in catalytic hydrolysis of EL and dealcoholization of EHP, which are two possible reaction pathways involved in the process. (Table S4 in ESI†). The results suggest that a minute increase in the hydrolysis rate of EL was observed when niobia was loaded. In another experiment, the trend of the dealcoholization activity from EHP to GVL follows: 10Nb-500-AC (90%) > 10Nb-300-AC (86%) > 10Nb-700-AC (56%) > AC (51%). This trend is very similar to that of the acidity determined by NH<sub>3</sub>-TPD, meaning that the surface acidity is essential for the GVL formation. It should be noted that though 10Nb-700-AC showed negligible NH<sub>3</sub> desorption in TPD measurement, it still showed excellent activity in dealcoholization of EHP and as a co-catalyst in EL hydrogenation in aqueous solution. This unexpected behavior in aqueous solution of Nb-700-AC is probably related to its NbO<sub>4</sub> tetrahedra of Nb<sub>2</sub>O<sub>5</sub>·*x*H<sub>2</sub>O with water-tolerant acidic properties as reported by Hara and co-workers.<sup>50</sup> We consider that the acidity of niobia hydrate may not be concisely justified by NH<sub>3</sub>-TPD and further studies should be carried out to clarify the acid catalyzed mechanism of niobia-involved reactions in aqueous solution.

#### Catalyst reusability

Given the excellent performance of 3Pd-10Nb-500-AC in hydrogenation, its reusability was also of interest from the viewpoint of practical application. After the first run, the cata-

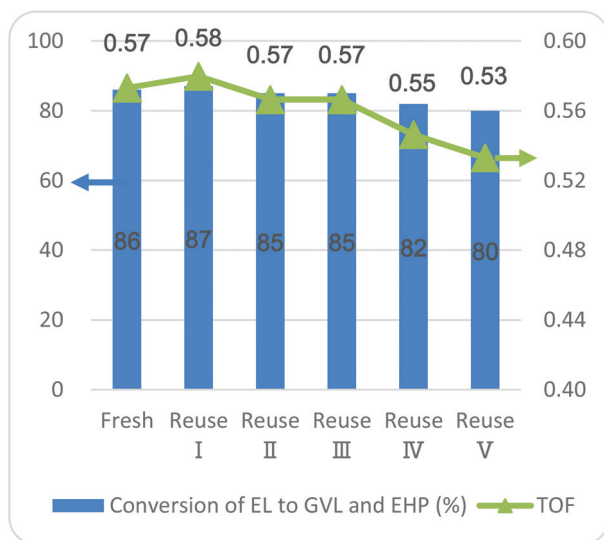


**Fig. 6** Recycle study of 3Pd-10Nb-500-AC in EL hydrogenation. Reaction conditions: 10 ml of 0.25 M EL aqueous solution; 0.5 MPa H<sub>2</sub>; 100 °C; 25 mg catalyst (3 wt% Pd); 5 h; 800 rpm. The TOF is defined as mol<sub>GVL+EHP</sub> g<sub>Pd</sub><sup>-1</sup> h<sup>-1</sup>.

lyst was separated through centrifugation, thoroughly washed and then dried at 50 °C in a vacuum oven before the next use. The activity in terms of EL conversion is shown in Fig. 6. It can be clearly seen that the 3Pd-10Nb-500-AC catalyst showed very stable reactivity in the first 4 runs and starts to deactivate in the next two runs. EL conversion of 80% was achieved in the 6th run. Chemisorption measurement suggested that the Pd dispersion was 59% for the spent sample, slightly decreased in comparison with the fresh one (65%, Table 2). An SEM-EDX study on the spent catalyst (not shown) was conducted and a negligible change of Pd content was observed. For comparison, the reusability of Pd-AC was also tested and the results are shown in Fig. 7. EL conversion on 3Pd-AC remained constant in the first 3 runs and then significantly decreased in the next 2 runs. CO chemisorption result suggested a remarkable decrease of Pd dispersion 53% (fresh) to 32% after 5 runs (Table 2). This result demonstrates the importance of niobia species in stabilizing Pd during the hydrogenation process.<sup>29,44,51</sup>

### Ring-opening of GVL

Lange *et al.*<sup>40</sup> disclosed the production of pentanoate (PA) based biofuels from LA *via* hydrogenation in different alcohols. To this end, a multifunctional Pt catalyst was employed, wherein Pt-TiO<sub>2</sub> catalyzing LA hydrogenation to GVL and zeolite (*i.e.* H-ZSM-5) catalyzing the GVL ring-opening to PA and esterification of PA to give ethyl pentanoate (PE). In this case, a 70% yield of PA was achieved with a Pt-H-ZSM-5-SiO<sub>2</sub> catalyst.<sup>52</sup> This process could also be performed in a one-pot reaction from ethyl levulinate (EL) over the Ru-H-β-silica catalyst, with PA and PE yield of 62%.<sup>53</sup> In our work, ring-opening reaction of GVL to PE was performed with GVL (10 mmol) in EtOH (100 mmol) over 3Pd-10Nb-500-AC catalysts (100 mg).

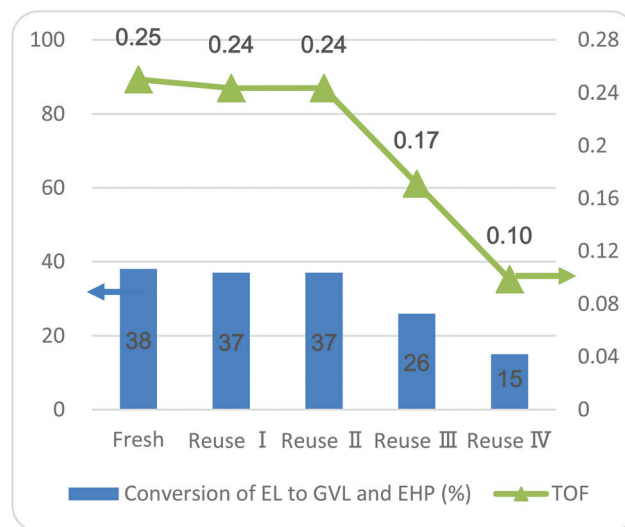


**Fig. 7** Recycle study of 3Pd-AC in EL hydrogenation. Reaction conditions: 10 ml of 0.25 M EL aqueous solution; 0.5 MPa H<sub>2</sub>; 100 °C; 25 mg catalyst (3 wt% Pd); 5 h; 800 rpm. The TOF is defined as mol<sub>GVL+EHP</sub> g<sub>Pd</sub><sup>-1</sup> h<sup>-1</sup>.

The reaction was conducted in a 50 mL autoclave at 250 °C for 10 h using a hydrogen pressure of 20 bar and a stirring speed of 300 rpm. A 70% yield of PE was obtained. This result suggested that Nb doped Pd nanoparticle showed similar reactivity to Pt and Ru in PE production from GVL or EL, thereby showing promising practical application in future biomass conversion.

## Conclusions

We demonstrated that the hydrogenation of aqueous ethyl levulinate to γ-valerolactone can be successfully performed under mild conditions over the Pd-AC catalyst doped with Nb<sub>2</sub>O<sub>5</sub>. Unlike bulk Nb<sub>2</sub>O<sub>5</sub>, the homogeneously dispersed Nb<sub>2</sub>O<sub>5</sub> plays a bifunctional role in stabilizing the Pd nanoparticles in the range of 1.4–2.5 nm and acting as an acidic promoter enhancing the formation of GVL from both EL and LA. The promoting effect of Nb<sub>2</sub>O<sub>5</sub> is dependent on the surface loading and calcination temperature during the preparation. The highest reactivity was found for 3 wt% Pd supported on 10 wt% Nb<sub>2</sub>O<sub>5</sub>-AC calcined at 500 °C, with GVL yield of 81% at 100 °C under a substrate-Pd mole ratio of 355. Furthermore, this catalyst can catalyze the conversion of GVL to PE in ethanol. Our studies showed important implications for the development of catalysts for bio-renewable conversions.

## Acknowledgements

We acknowledge the financial support from the National Natural Science Foundation of China (grant no. 21203065) and the Fundamental Research Funds for the Central Universities.

## Notes and references

- E. I. Gurbuz, D. M. Alonso, J. Q. Bond and J. A. Dumesic, *ChemSusChem*, 2011, **4**, 357.
- A. J. J. E. Eerhart, W. J. J. Huijgen, R. J. H. Grisel, J. C. van der Waal, E. de Jong, A. de Sousa Dias, A. P. C. Faaij and M. K. Patel, *RSC Adv.*, 2014, **4**, 3536.
- H. Rasmussen, H. R. Sorensen and A. S. Meyer, *Carbohydr. Res.*, 2014, **385**, 45.
- D. M. Alonso, S. G. Wettstein and J. A. Dumesic, *Green Chem.*, 2013, **15**, 584.
- J. Q. Bond, D. M. Alonso, D. Wang, R. M. West and J. A. Dumesic, *Science*, 2010, **327**, 1110.
- I. T. Horvath, H. Mehdi, V. Fabos, L. Boda and L. T. Mika, *Green Chem.*, 2008, **10**, 238.
- D. Cerniauskaite, J. Rousseau, A. Sackus, P. Rollin and A. Tatibouet, *Eur. J. Org. Chem.*, 2011, 2293.
- R. H. Guo, Q. Zhang, Y. B. Ma, X. Y. Huang, J. Luo, L. J. Wang, C. A. Geng, X. M. Zhang, J. Zhou, Z. Y. Jiang and J. J. Chen, *Bioorg. Med. Chem.*, 2011, **19**, 1400.
- Z. Ma, Y. Hong, D. M. Nelson, J. E. Pichamuthu, C. E. Leeson and W. R. Wagner, *Biomacromolecules*, 2011, **12**, 3265.
- I. van der Meulen, E. Gubbels, S. Huijser, R. Sablong, C. E. Koning, A. Heise and R. Duchateau, *Macromolecules*, 2011, **44**, 4301.
- L. E. Manzer, *Appl. Catal., A*, 2004, **272**, 249.
- P. G. Jessop, *Green Chem.*, 2011, **13**, 1391.
- D. Fegyverneki, L. Orha, G. Láng and I. T. Horváth, *Tetrahedron*, 2010, **66**, 1078.
- Z. Yang, Y. B. Huang, Q. X. Guo and Y. Fu, *Chem. Commun.*, 2013, **49**, 5328.
- M. G. Al-Shaal, W. R. H. Wright and R. Palkovits, *Green Chem.*, 2012, **14**, 1260.
- A. M. R. Galletti, C. Antonetti, V. De Luise and M. Martinelli, *Green Chem.*, 2012, **14**, 688.
- W. R. Wright and R. Palkovits, *ChemSusChem*, 2012, **5**, 1657.
- A. M. Hengne and C. V. Rode, *Green Chem.*, 2012, **14**, 1064.
- W. Li, J.-H. Xie, H. Lin and Q.-L. Zhou, *Green Chem.*, 2012, **14**, 2388.
- M. Chia and J. A. Dumesic, *Chem. Commun.*, 2011, **47**, 12233.
- H. N. Pham, Y. J. Pagan-Torres, J. C. Serrano-Ruiz, D. Wang, J. A. Dumesic and A. K. Datye, *Appl. Catal., A*, 2011, **397**, 153.
- X. L. Du, Q. Y. Bi, Y. M. Liu, Y. Cao and K. N. Fan, *ChemSusChem*, 2011, **4**, 1838.
- L. Deng, Y. Zhao, J. Li, Y. Fu, B. Liao and Q. X. Guo, *ChemSusChem*, 2010, **3**, 1172.
- L. Deng, J. Li, D. M. Lai, Y. Fu and Q. X. Guo, *Angew. Chem., Int. Ed.*, 2009, **48**, 6529.
- H. Mehdi, V. Fabos, R. Tuba, A. Bodor, L. T. Mika and I. T. Horvath, *Top. Catal.*, 2008, **48**, 49.
- R. A. Bourne, J. G. Stevens, J. Ke and M. Poliakoff, *Chem. Commun.*, 2007, 4632.
- J. P. Lange, J. Z. Vestering and R. J. Haan, *Chem. Commun.*, 2007, 3488.
- M. Chalid, A. A. Broekhuis and H. J. Heeres, *J. Mol. Catal. A: Chem.*, 2011, **341**, 14.
- R. Buitrago-Sierra, J. C. Serrano-Ruiz, F. Rodriguez-Reinoso, A. Sepulveda-Escribano and J. A. Dumesic, *Green Chem.*, 2012, **14**, 3318.
- S. G. Wettstein, J. Q. Bond, D. M. Alonso, H. N. Pham, A. K. Datye and J. A. Dumesic, *Appl. Catal., B*, 2012, **117–118**, 321.
- P. P. Upare, J.-M. Lee, D. W. Hwang, S. B. Halligudi, Y. K. Hwang and J.-S. Chang, *J. Ind. Eng. Chem.*, 2011, **17**, 287.
- H. Heeres, R. Handana, D. Chunai, C. Borromeus Rasrendra, B. Girisuta and H. Jan Heeres, *Green Chem.*, 2009, **11**, 1247.
- L. E. Manzer, *WO 2002074760A1*, 2002.
- M. J. Climent, A. Corma and S. Iborra, *Green Chem.*, 2014, **16**, 516.
- L. Peng, L. Lin, J. Zhang, J. Shi and S. Liu, *Appl. Catal., A*, 2011, **397**, 259.
- B. C. Windom, T. M. Lovestead, M. Mascall, E. B. Nikitin and T. J. Bruno, *Energy Fuels*, 2011, **25**, 1878.
- B. Kim, J. Jeong, S. Shin, D. Lee, S. Kim, H. J. Yoon and J. K. Cho, *ChemSusChem*, 2010, **3**, 1273.
- X. Hu and C. Z. Li, *Green Chem.*, 2011, **13**, 1676.
- K.-i. Tominaga, A. Mori, Y. Fukushima, S. Shimada and K. Sato, *Green Chem.*, 2011, **13**, 810.
- J. P. Lange, R. Price, P. M. Ayoub, J. Louis, L. Petrus, L. Clarke and H. Gosselink, *Angew. Chem., Int. Ed.*, 2010, **49**, 4479.
- J. M. Nadgeri, N. Hiyoshi, A. Yamaguchi, O. Sato and M. Shirai, *Appl. Catal., A*, 2014, **470**, 215.
- H. Xiong, T. Wang, B. H. Shanks and A. K. Datye, *Catal. Lett.*, 2013, **143**, 509.
- H. Xiong, H. N. Pham and A. K. Datye, *J. Catal.*, 2013, **302**, 93.
- H. Xiong, M. Nolan, B. H. Shanks and A. K. Datye, *Appl. Catal., A*, 2014, **471**, 165.
- G. S. Nair, E. Adrijanto, A. Alsalmeh, I. V. Kozhevnikov, D. J. Cooke, D. R. Brown and N. R. Shiju, *Catal. Sci. Technol.*, 2012, **2**, 1173.
- T. Iizuka, K. Ogasawara and K. Tanabe, *Bull. Chem. Soc. Jpn.*, 1983, **56**, 2927.
- I. Nowak and M. Ziolkowski, *Chem. Rev.*, 1999, **99**, 3603.
- K. Yan, T. Lafleur and J. Liao, *J. Nanopart. Res.*, 2013, **15**, 1906.
- K. Yan, T. Lafleur, G. Wu, J. Liao, C. Ceng and X. Xie, *Appl. Catal., A*, 2013, **468**, 52.
- K. Nakajima, Y. Baba, R. Noma, M. Kitano, J. N. Kondo, S. Hayashi and M. Hara, *J. Am. Chem. Soc.*, 2011, **133**, 4224.
- W. Luo, U. Deka, A. M. Beale, E. R. H. van Eck, P. C. A. Bruijninx and B. M. Weckhuysen, *J. Catal.*, 2013, **301**, 175.
- J.-P. Lange, *US Patent 2011/0112326*, 2011.
- P. J. van den Brink, K. L. Von Hebel, J.-P. Lange and L. Petrus, *WO/2006/[067171]*, 2006.